DYNA
http://dyna.medellin.unal.edu.co/

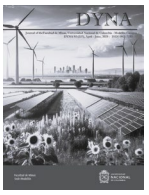

UNIVERSIDAD NACIONAL DE COLOMBIA

A low-cost upper limb exoskeleton assistive device based on elbow torque feedback

Jiaxin Huang †, Fan Wu †, Baoyi Ding, Jiasheng Yin,
Guang Yang & Zhigong Song *

*Jiangsu Provincial Key Laboratory of Food Advanced Manufacturing Equipment Technology, School of Mechanical Engineering, Jiangnan University, Wuxi China. 6230811010@stu.jiangnan.edu.cn, 1043220119@stu.jiangnan.edu.cn, 1044220401@stu.jiangnan.edu.cn, 1042220122@stu.jiangnan.edu.cn, 1042220119@stu.jiangnan.edu.cn, *Corresponding author: song_jnu@jiangnan.edu.cn*
†These authors contributed equally to this work

Received: February 3rd, 2025. Received in revised form: April 25th, 2025. Accepted: May 16th, 2025

Abstract
To alleviate upper limb movement impairment in specific groups, reduce the heavy workload of laborers, and assist patients with elbow joint injuries in post-rehabilitation training, we designed a wearable upper limb exoskeleton. A dual-motor system based on elbow torque feedback can realize the smooth rotation and motion assistance of elbow joints by motor driving. To evaluate the performance of the upper limb exoskeleton, we conducted a loaded elbow flexion comparative test while collecting and evaluating electromyographic (EMG) signals. The test demonstrates that the upper limb exoskeleton effectively abates muscle workload. This low-cost upper limb exoskeleton effectively assists movement and enhances upper limb endurance for rehabilitation training or tasks like lifting and carrying. It offers an opportunity to enhance the quality of life for users by aiding in the recovery or improvement of upper limb function.

Keywords: upper limb exoskeleton; torque feedback; loaded elbow flexion; EMG signals; performance evaluation.

Un dispositivo de asistencia del exoesqueleto de las extremidades superiores de bajo costo basado en la retroalimentación del torque del codo

Resumen
Para aliviar el deterioro del movimiento de las extremidades superiores en grupos específicos, reducir la gran carga de trabajo de los trabajadores, y ayudar a los pacientes con lesiones en las articulaciones del codo en el entrenamiento post-rehabilitación, hemos diseñado un exoesqueleto vestible de las extremidades superiores. Un sistema de doble motor basado en la retroalimentación del par del codo puede realizar la rotación suave y la asistencia de movimiento de las articulaciones del codo por motor de conducción. Para evaluar el desempeño del exoesqueleto del miembro superior, se realizó un test comparativo de flexión del codo cargado mientras se recogían y evaluaban las señales electromiográficas (EMG). La prueba demuestra que el exoesqueleto del miembro superior disminuye con eficacia la carga de trabajo muscular. Este exoesqueleto de las extremidades superiores de bajo costo ayuda eficazmente al movimiento y mejora la resistencia de las extremidades superiores para el entrenamiento de rehabilitación o tareas como levantar y llevar. Ofrece una oportunidad para mejorar la calidad de vida de los usuarios al ayudar en la recuperación o mejora de la función de las extremidades superiores.

Palabras clave: exoesqueleto del miembro superior; retroalimentación de par; flexión del codo con carga; las señales EMG; evaluación del desempeño.

1. Introduction

With the progress of population aging, the number of the elderly suffering from upper limb functional impairments is increasing, driving higher demand for corresponding social security and medical resources. In recent years, assistive

How to cite: Huang†, J., Wu†, F., Ding, B., Yin, J., Yang, G., and Song, Z., A low-cost upper limb exoskeleton assistive device based on elbow torque feedback. DYNA, 92(237), pp. 96-105, April - June, 2025.

exoskeletons have been extensively studied as a viable rehabilitation solution. By providing targeted assistance and movement control, exoskeleton systems facilitate the restoration and enhancement of upper limb motor functions in patients, demonstrating significant potential for clinical application and cost-effectiveness [1]. Although industries are undergoing digital and intelligent upgrades, with the widespread adoption of intelligent manufacturing, digital workshops, unmanned production lines and intelligent equipment, frontline workers are still responsible for a significant amount of high-intensity physical labor due to the increasing specificity of industrial demands. Exoskeleton can significantly mitigate the health risks of such labor, effectively alleviating muscle and cardiac fatigue, and ultimately helping to prevent occupational diseases. Additionally, these devices enhance efficiency and quality in repetitive tasks, leading to a more optimized work environment in factories.

The high demand for exoskeleton robots has garnered the attention of researchers worldwide. For example, the Swiss Federal Institute of Technology Zurich developed the fully actuated upper limb exoskeleton ANYexo 2.0 [2], designed for joint-oriented training across all stages of rehabilitation. This exoskeleton is equipped with 9 degrees of freedom (DoF) under active control and 3 six-DoF force/torque sensors, enabling it to seamlessly track the upper limb's movements. It is designed as a highly adaptable therapeutic robot, capable of serving a broad range of users and exercises. However, its high energy consumption and cost limit its widespread use. Similarly, the "Carry" pneumatic elbow exoskeleton, designed by the Technical University of Munich [3], is a lightweight, active device primarily designed to assist with carrying tasks. It can relieve localized muscle fatigue; however, its complex pneumatic components may make maintenance challenging and time-consuming.Exoskeletons with flexible assistance can also be driven by tendons, such as the Myoshirt textile exomuscle from the Swiss Federal Institute of Technology Zurich [4], which helped testers delay muscle fatigue onset by 51.5 seconds and reduce muscle activity by 49.1%. Moreover, the Series Elastic Actuator (SEA) is a widely used type of joint actuator for exoskeletons [5,6]. To ensure ease of use, exoskeleton actuators need to be lightweight and compact while still meeting performance requirements. In addition to active assistance methods, passive exoskeletons also exist. One example is the unpowered ankle exoskeleton developed by Carnegie Mellon University [7]. It uses ratchets and springs to passively support human movement.

Improving the comfort and portability of exoskeletons is a challenge in human motion assistance [8], requiring solutions to technical problems like motion compatibility and the development of effective human-machine interaction [9]. The choice of actuation method is crucial. In this study, we adopt direct motor drive assistance, which offers high efficiency, rapid response, low maintenance requirements and precise control. In the design of upper limb exoskeletons, torque feedback [10,11] is a key technology that detects the user's motion intent and provides torque compensation, facilitating more precise replication and enhancement of upper limb functions through personalized assistance. The elbow joint is among the most complex joints in the upper limb, characterized by a broad range of motion and diverse functions [12]. Through elbow torque feedback, the exoskeleton can more accurately mimic and enhance the user's elbow function, allowing them to carry out more daily activities and work tasks [13]. However, research on elbow torque feedback remains relatively limited, primarily concentrating on algorithms and control strategies while often overlooking user experience and adaptability. Therefore, this paper seeks to enhance the design and performance of upper limb exoskeleton assistive devices by investigating elbow torque feedback technology. The goal is to deliver improved assistance and user experience while designing a low-cost upper limb exoskeleton. This paper outlines the principles and mechanisms of upper limb exoskeleton robots, covering structural design, torque computation and torque feedback control. The experimental procedures and performance evaluations are thoroughly presented to assess the efficacy and functionality of the exoskeleton device. This work aims to guide and inspire the design and implementation of upper limb exoskeleton assistive devices while encouraging further research and advancement in elbow torque feedback technology. This will enhance the rehabilitation experience and work quality for individuals undergoing rehabilitation training or performing heavy-lifting tasks, aiding in the recovery or improvement of their upper limb motor function. We created the exoskeleton Project Website: https://exoskeleton-club.github.io/ULETF/.

2. Mechanical design of the upper limb exoskeleton

2.1 Structural design

This section introduces the bionic design of the upper limb exoskeleton structure, replicates the freedom of the human upper limb, and provides flexible rotational freedom for each joint and controllable auxiliary torque for the elbow joint. The exoskeleton is composed of three sub-modules: the back, shoulders and elbows. The main degrees of freedom in the upper limbs come from the shoulder, elbow and wrist joints, which exert force on the shoulder and elbow muscles when carrying objects or lifting heavy objects, especially during flexion/extension. To reduce weight and improve control, the shoulder joint features passive support, while the elbow joint is driven by a direct motor. We replaced the traditional reducer with a direct-drive system, allowing the exoskeleton joints to be controlled by the user's movements [11] and eliminating the need for complex trajectory planning.

When the exoskeleton system's degrees of freedom match those of the human body, it offers maximum comfort and unrestricted movement. However, from a control perspective, fewer degrees of freedom make the system easier to manage, creating a trade-off between control feasibility and comfort. To balance both control and comfort, this exoskeleton is primarily designed to support the shoulder and elbow joints. Considering both control ease and freedom matching, the shoulder joint was assigned 3 degrees of freedom, the elbow joint 1 degree of freedom, while the wrist joint was omitted, resulting in a total of 4 degrees of freedom for the right upper limb.

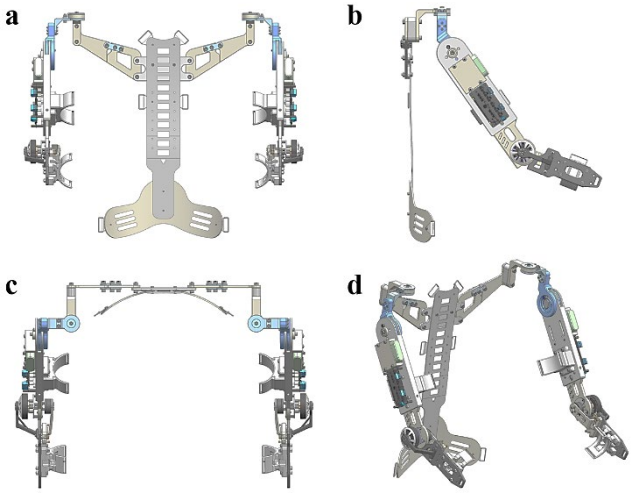

Figure 1. Structural design of upper limb exoskeleton. (a) The front view of the exoskeleton. (b) The left view of the exoskeleton. (c) The top view of the exoskeleton. (d) The axonometric diagram of the exoskeleton.
Source: authors

This setup is sufficient to meet the needs of most activities of daily living (ADLs) [14], while maintaining workspace integrity and simplifying both structure and control. The exoskeleton's weight is distributed through the back plate, and when integrated with a lower limb exoskeleton, it can be further transferred to the ground. The 3D structural design is illustrated in Fig. 1.

Fig. 1 shows the three orthographic views and an axonometric projection of the upper limb exoskeleton robot. The backplate features buckles, while the ring supports on the upper and lower arm panels include slots for securing them to the body with straps, elastic bands and Velcro. The length of the upper arm panel is adjustable to accommodate users of different heights. The elbow joint incorporates a dual-motor coaxial design, while the back panel is constructed from rigid aluminum alloy to provide support. The exoskeleton joint axis must align with the user's joint axis to ensure movement coordination. To lower manufacturing costs and simplify production, most exoskeleton components are fabricated from 3D-printed white resin.

2.2 Range of motion of the upper limb joints

The design of the exoskeleton structure must ensure that the dimensions of the parts and the joint constraints align with the range of motion of the human upper limb. The motion range of the exoskeleton joints should be defined according to the normal range of human joint motion. The shoulder joint is the most complex joint in the upper limb, with three orthogonal rotational degrees of freedom: abduction/adduction about axis-1, external/internal rotation about axis-2 and flexion/extension about axis-3. The elbow joint rotates about axis-4 and is considered to have one degree of freedom: flexion and extension. The wrist joint is the most complex joint in the upper limb, which can also be simplified into three rotational DOFs [14]. As the exoskeleton design excludes the wrist joint, the human wrist's range of motion is not considered. After analyzing the DOF of the upper limb, the motion angles of each joint need to be studied to design appropriate joint motion ranges and limits. Aligning the exoskeleton design with the range of motion of the human upper limb enhances both practicality and comfort. The specific joint limits, detailed structural information, and simplified diagram of human joint freedom corresponding to the exoskeleton are shown in Fig. 2.

The elbow joint of the upper limb exoskeleton incorporates a mechanical limiter, restricting the motion angle to 0°–130° (Fig. 2a). Fig. 2b illustrates the adjustable mechanism of the upper arm plate, where the length can be modified by changing the hole position and bolt connection. The forearm plate measures 200 mm, while the upper arm

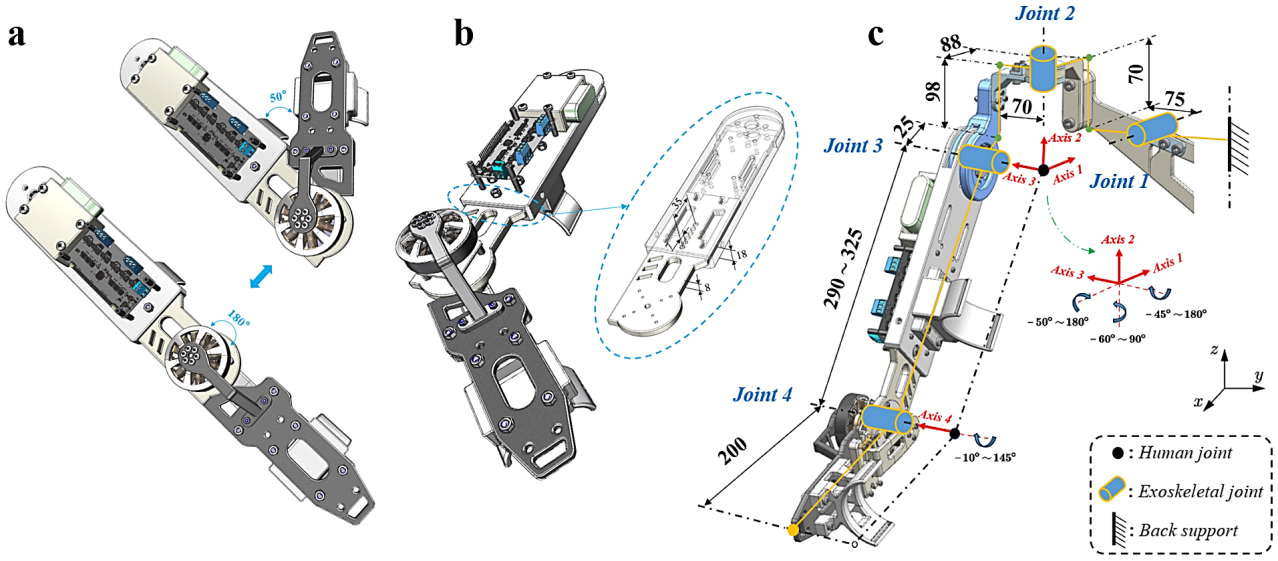

Figure 2. Joint limitations in upper limb exoskeleton with partial details and diagrammatic diagram of human joint freedom. (a) Variation of the joint limiting angle at the elbow joint of the exoskeleton. (b) Detail of the assembly of the adjustable plate of the exoskeleton with the big arm plate. (c) Diagram of the degrees of freedom of the human body joints in the positions corresponding to the joints of the exoskeleton.
Source: authors

Table 1.
The range of joint movement restrictions of the exoskeleton.

Axis	Angle Range	Joint/Assistance Type
Axis-1	0° ~ 180°	Shoulder [Abduction/Adduction] (Passive Support)
Axis-3	-55° ~ 30°	Shoulder [External/Internal Rotation] (Passive Support)
Axis-3	-40° ~ 140°	Shoulder [Flexion/Extension] (Passive Support)
Axis-4	0° ~ 130°	Elbow [Flexion/Extension] (Direct Motor Drive)

Source: authors

plate is adjustable between 290 mm and 325 mm. The simplified DOF of human joints include 3-DOF for the shoulder and 1-DOF for the elbow, corresponding to upper limb shoulder abduction/adduction (axis-1), external/internal rotation (axis-2), flexion/extension (axis-3) and elbow flexion/extension (axis-4) [14]. The defined zero angles correspond to the arm positioned perpendicular to the ground, as illustrated in Fig. 2c. The right-hand rule was applied to determine the positive and negative rotation angles of the joints, representing the normal motion range of the upper limb joints. Upon determining the normal range of motion for human upper limb joints, the rotational limits of the exoskeleton joints can be precisely defined. These constraints are enforced via mechanical stoppers, with the joint motion ranges of the exoskeleton manually specified. The joint motion limits and corresponding constraints of the exoskeleton are shown in Table 1.

The range of joint motion limitations in the exoskeleton is a key design consideration to prevent the user's movements from exceeding physiological boundaries. This design improves user safety and comfort while enhancing operational efficiency. The mechanical structure's constraints precisely regulate joint motion, ensuring effective protection for human joints.

1. Upper limb exoskeleton elbow joint control

1.1 Torque estimation

When assisting the movement of the human elbow joint with the upper limb exoskeleton, careful consideration must be given to the configuration and selection of the assistive motor. A motor that is too small will provide insufficient assistance, while an overly large motor adds unnecessary weight and bulk, diminishing comfort by increasing inertia. Torque estimation at the exoskeleton joint is essential to evaluate the assistive effect and the motor's self-weight. For example, during arm-lifting movements, the torque reaches its peak when the upper arm and forearm are fully extended horizontally. This posture serves as the baseline for joint torque calculations. The state diagram of the exoskeleton in the maximum force-arm position, finite element analysis (FEA) of key components and the control block diagram for position mode are shown in Fig. 3.

The specific state diagram for the upper limb in the maximum force-arm position is shown in Fig. 3a. In Fig. 3, T_1 represents the torque at the shoulder joint

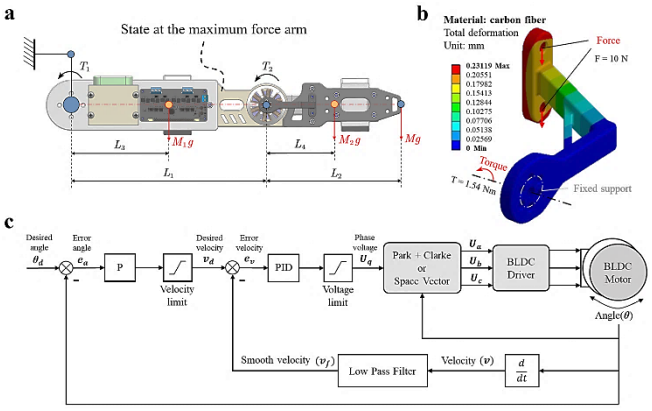

Figure 3. State diagram at the maximum force arm of the upper limb exoskeleton with finite element analysis of key components and control block diagram of the position mode. (a) State diagram at the maximum force arm giving the force analysis. (b) Finite element analysis of key component of the upper limb exoskeleton. (c) Control block diagram of exoskeleton motor position control.
Source: authors

(flexion/extension), and T_2 represents the torque at the elbow joint (flexion/extension). L_1 denotes the length of the exoskeleton's upper arm, $L2$ the length of the forearm (excluding the wrist), L_3 the distance from the center of mass of the upper arm to the shoulder joint, and $L4$ the distance from the center of mass of the forearm to the elbow joint. M_1g represents the weight of the exoskeleton's upper arm, and M_2g represents the weight of the forearm. Mg refers to the compensatory weight at the distal end of the exoskeleton's upper limb. Based on the theorem of static equilibrium, torque can be calculated at the elbow and shoulder joint centers. See eq. (1) and eq. (2):

$$T_2 = Mg \times L_2 + M_2g \times L_4 \tag{1}$$

$$T_1 = Mg \times (L_1 + L_2) + M_2g \times (L_1 + L_4) + M_1g \times L_3 - T_2 \tag{2}$$

After assigning values to the parameters, we obtain the following dimensions from measurements: L_1 =339mm, L_2 =200mm, L_3 = 157mm, L_4 = 96mm, M_1 = 0.5kg, M_2 = 0.4kg. The compensatory mass M of the upper limb is set to 0.6kg, and the gravitational acceleration，g = 9.8N/kg. Substituting these values into the formulas yields T_1 = 4.09Nm, T_2 = 1.55Nm. Thus, the torque required for the assistive motor at the elbow joint must be close to 1.55Nm. As the shoulder joint is supported passively, the necessary torque is compensated entirely by the passive support structure, with no need for active motor assistance. The shoulder joint's three degrees of freedom are supported by mechanical structures containing rolling bearings, ensuring smooth rotation of the exoskeleton's shoulder joint.

The key distinction between an assistive exoskeleton system and other robots lies in the fact that the operator is a human, not the machine. The operator is part of the control

loop, meaning the human is "in the loop". The operator and the exoskeleton interact physically, forming a tightly coupled human-machine system. The objective of controlling this coupled system is to facilitate seamless coordination between the human and machine to accomplish tasks. A key advantage of direct-drive assistance is that it keeps the assistive joints lightweight, eliminating the need for traditional robotic motion planning. The exoskeleton's joint motion only needs to mirror the real-time movements of the human body. When the human body remains stable, the exoskeleton can maintain its stability without requiring additional control, relying entirely on the human body for balance.

1.2 Torque feedback

Based on torque estimation, a 5008-400KV brushless DC (BLDC) motor was chosen as the assistive motor for the exoskeleton's elbow joint. The motor provides a rated torque of 1.54 Nm and a power output ranging from 28.1 to 355.2 W, satisfying the assistive requirements for the elbow joint. A small gimbal motor served as the drive motor, sharing the same axis with the assistive motor. As the elbow bends or extends, the human body exerts a slight torque to activate the drive motor, which operates coaxially with the assistive motor to generate torque feedback. Both motors output torque synchronously, with the assistive motor driving the forearm panel to provide elbow assistance. The elbow control system includes a position sensor, eliminating the need for a position observer.

The Space Vector Pulse Width Modulation (SVPWM) serves as the final execution part of Field-Oriented Control (FOC) [15], receiving the $V\alpha$ and $V\beta$ signals from the FOC to control the stator windings and generate a rotating magnetic field.

The core principle of torque feedback in this exoskeleton robot is to utilize the angular difference between the two motors as the target value in torque mode, ensuring that the angular difference is driven to zero. As one motor rotates, the other generates torque to track and follow the movement. Similarly, when one motor stalls, the other motor halts as the angular difference converges to the stalled motor's angle. Torque feedback eliminates the need for current sampling and can be implemented using voltage mode, which is ideal for low-speed motor control with rapid execution response. Finally, the dual-motor torque feedback control system diagram is shown in Fig. 4.

As shown in Fig. 4c, when the upper limb muscles contract, they generate a force $F_{muscle.}$ Due to the presence of a lever arm r between the muscle force and the joint's center of rotation, F_{muscle} produce a torque T_{muscle} that causes the joint to rotate.

If the forearm is extended, the biceps relax, and the muscles on the opposite side of the joint contract to pull the joint back to a horizontal position, where $T_{muscle} = F_{muscle} \times r_{\circ}$.
According to the control block diagram of the dual-motor torque feedback, when the deviation $e = \theta i - \theta o$ approaches zero, the total torque T_{joint} at the human elbow joint can be

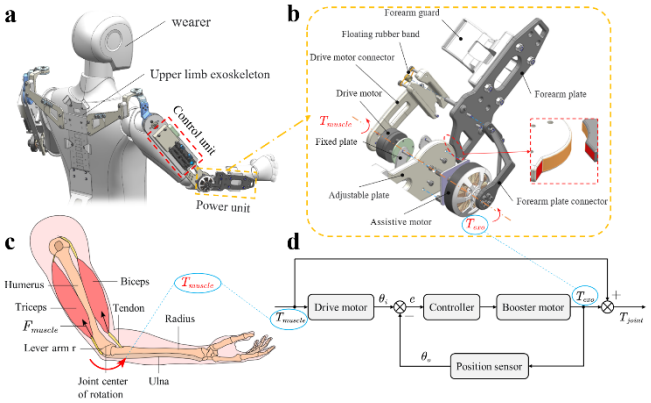

Figure 4. Schematic of the control system for dual-motor torque feedback at the elbow joint of the exoskeleton. (a) Schematic diagram of human wearing the upper limb exoskeleton. (b) Exploded view of the motor assembly at the elbow joint of the exoskeleton. (c) Schematic diagram of human upper limb muscles. (d) Block diagram of the control system at the elbow joint of the exoskeleton.
Source: authors

considered as the sum of the torque generated by the muscles T_{muscle} and the torque provided by the exoskeleton T_{exo}, $T_{joint} = T_{muscle} + T_{exo}$. The torque produced by the dual-motor feedback in the elbow of the exoskeleton is transmitted to the wearer via linkages. Ideally, this setup can reduce the load on human muscles. If the movement direction of the human body and the exoskeleton are aligned (which the control system ensures), the user can leverage the exoskeleton to perform tasks with less effort.

2. Performance evaluation of the exoskeleton

2.1 Preliminary performance evaluation

For performance evaluation [16-18] of the exoskeleton robot, four main aspects are considered: comfort, applicability, safety and reliability. Comfort can be assessed through human-machine interaction forces, muscle fatigue, appearance and noise; applicability can be evaluated through maximum load capacity, endurance and time required for donning and doffing; safety is measured by ensuring that the exoskeleton's range of motion is less than the physiological limits of the human body, with warning and protection mechanisms in place in the event of failure; and reliability can be assessed through the mean time between failures and average repair time.

The performance of this upper limb exoskeleton is evaluated based on two criteria: muscle fatigue and elbow flexion/extension angular velocity. Muscle fatigue is evaluated through electromyography (EMG). Surface electromyography (sEMG) is the composite effect of electrical activity from superficial muscles and nerve trunks on the skin's surface. It represents the bioelectrical changes in the neuromuscular system during voluntary and involuntary movements. These signals are captured, amplified, displayed and recorded as

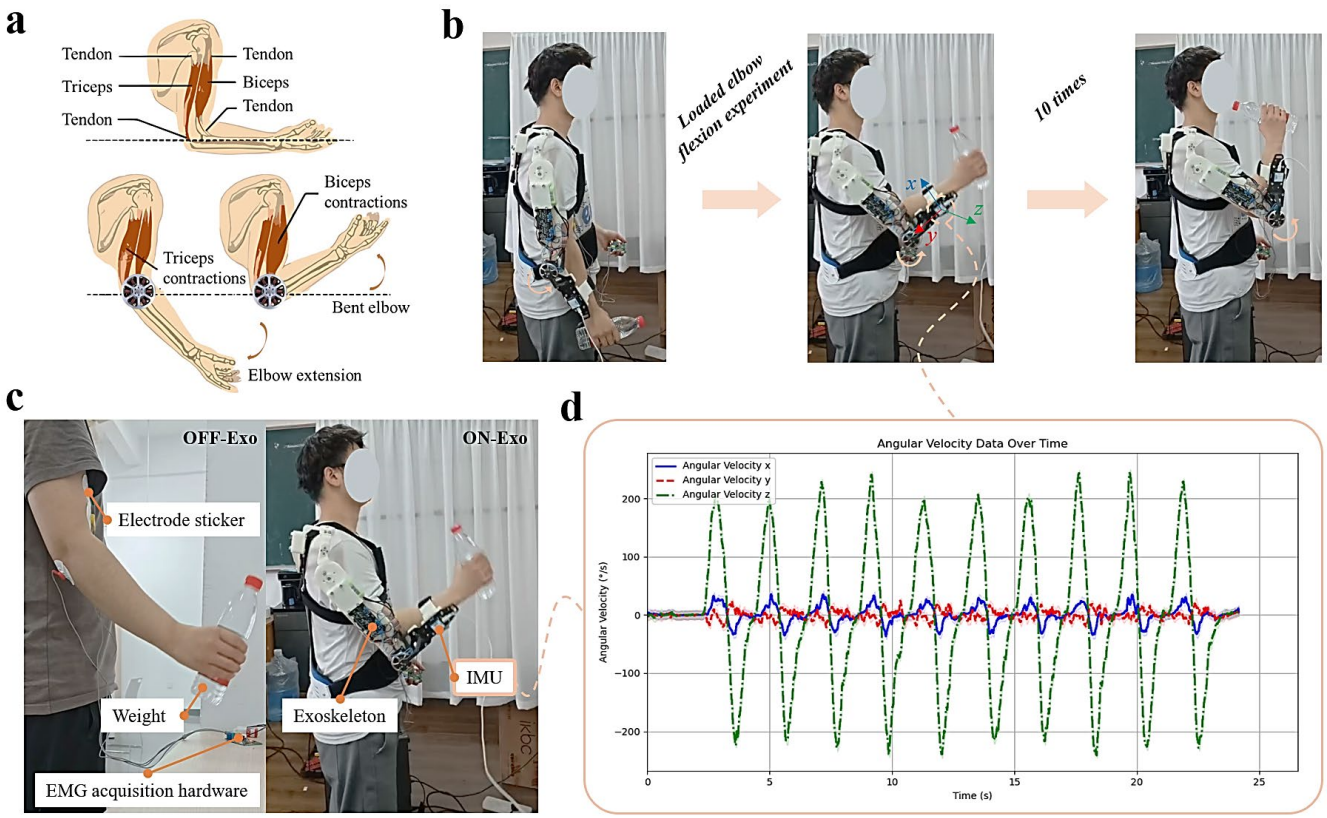

Figure 5. Performance evaluation of the upper limb exoskeleton. (a) Schematic diagram of human upper limb movement. (b) Motion processes in the upper limb exoskeleton. (c) Loaded elbow flexion experiment at the elbow joint. (d) Angular velocity data recording of IMU at the forearm in the upper limb exoskeleton.
Source: authors

one-dimensional voltage-time series through surface electrodes, providing a representation of neuromuscular activities to some extent. The preliminary performance evaluation experiment is a single-arm loaded elbow flexion test, during which EMG signals are collected using an EMG module to monitor changes in upper arm muscle activity. The experiment compares the muscle power output (especially of the biceps) during loaded elbow flexion with and without the exoskeleton. Performance evaluation of the exoskeleton as show in Fig. 5.

To reduce impedance and external interference during surface EMG signal collection, the subject's skin was cleaned with alcohol prior to data acquisition. The subject was a 23-year-old male, 176 cm tall, weighing 75 kg, and in good health. During the experiment, 10 single-arm loaded elbow flexions were performed, with the process of single-arm motion while wearing the upper limb exoskeleton shown in Fig. 5b. EMG signals were collected from the biceps brachii of the subject's upper arm to evaluate the performance of the exoskeleton. Ensuring consistent electrode placement on the same side and positioning them away from power sources is crucial to prevent 50 Hz power frequency interference. The specific experimental setup and hardware for EMG data collection are shown in Fig. 5c.

The angular velocity data from the IMU (Inertial Measurement Unit) sensor can be used to verify the effectiveness of the exoskeleton design, visually demonstrating the role of the exoskeleton in assistive motion. By analyzing the angular velocity of forearm movements, it is possible to evaluate the exoskeleton's impact on motion control and the efficiency of the wearer in performing specific tasks. Fig. 5d displays the angular velocity data recorded by the IMU at the forearm. In the performance evaluation of the exoskeleton, angular velocity data is used to assess the performance of the exoskeleton during specific tasks (such as the loaded elbow flexion experiment). Metrics include smoothness of motion, average speed and peak speed. Motion smoothness is assessed by calculating the standard deviation of angular velocity during movement. A lower standard deviation indicates less fluctuation around the mean, suggesting smoother movement and diminished oscillation. Average speed refers to the mean angular velocity during motion with the exoskeleton, reflecting the overall speed level. Peak speed represents the highest speed during movement, indicating the exoskeleton's capability to support rapid movements, particularly useful for tasks requiring quick responses.

From Fig. 5d, the smoothness (standard deviation) of Angular Velocity *x* is 13.88, the average speed is 9.70°/s, and the peak speed reaches 36.93°/s. This indicates smooth movement along the *x*-axis with moderate speed and quick responsiveness. For Angular Velocity *y*, the smoothness is 7.64, with an average speed of 5.83°/s and a peak speed of 24.41°/s. Compared to the *x*-axis, movements along the *y*-

axis are smoother with less fluctuation but slower, suggesting that the exoskeleton provides stable support in this direction. Angular Velocity z has a very high standard deviation of 122.29, an average speed of 94.12°/s and a peak speed of 243.71°/s. This indicates significant fluctuation along the z-axis (corresponding to elbow movements) and suggests that this is the most active direction of motion, reflecting the upper limb exoskeleton's high responsiveness in supporting rapid movements.

Using EMG hardware and an upper computer for data collection, a single-arm loaded elbow flexion experiment (10 repetitions) was performed, comparing the EMG data collected with and without wearing the exoskeleton (OFF-Exo and ON-Exo). The data collected by the upper computer was imported into Excel for basic processing, followed by electromyography signal analysis using Python. A sampling rate of 1000 was set during filtering, and band-pass filtering was applied to obtain the filtered EMG signals, with low and high cutoff frequencies set to 10 Hz and 450 Hz, respectively. The filtered signal and corresponding smoothed envelopes are shown in Fig. 6, with the vertical axis representing muscle EMG intensity. From the EMG signal envelopes in Fig. 6, it is evident that the EMG intensity is lower in the ON-Exo condition compared to the OFF-Exo condition.

Next, time-domain features of the EMG signals were extracted to provide a comparison, using two relatively stable metrics: root mean square (RMS) and average rectified value (aEMG). See eq. (3) and eq. (4).

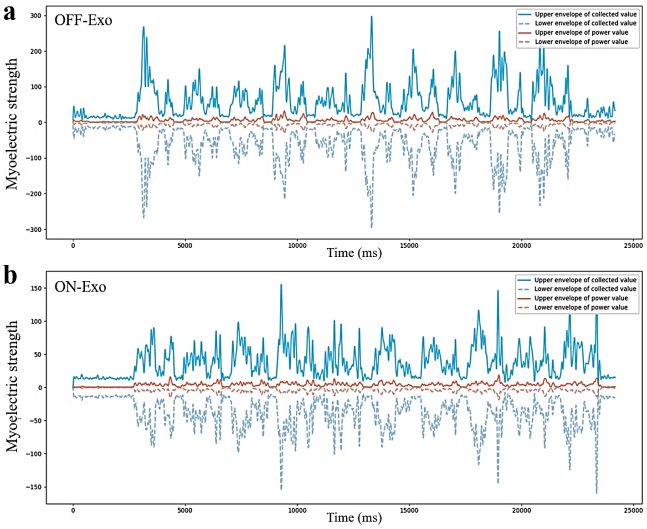

Figure 6. Comparison of the envelope of the filtered EMG signal after the experimental collection. (a) EMG signal envelope (OFF-EXO) during loaded elbow flexion experiments without wearing the upper limb exoskeleton. (b) EMG signal envelope (ON-EXO) during loaded elbow flexion experiments while wearing the upper limb exoskeleton.
Source: authors

$$\mathrm{RMS} = \sqrt{\frac{1}{N}\sum_{i=1}^{N} x^2(i)} \tag{3}$$

The formula for calculating aEMG is:

$$\mathrm{aEMG} = \frac{1}{N}\sum_{i=1}^{N} |x(i)| \tag{4}$$

Where N represents the total number of samples in the discrete time series x, and i represents the i-th discrete time point. The time-domain feature extraction of EMG power values is shown in Table 2.

In the time-domain feature comparison of EMG, each value in the ON-Exo condition is lower than the corresponding value in the OFF-Exo condition. Specifically, the RMS of the collected values decreased by 41.61%, and the aEMG decreased by 35.79%. The RMS of the power values decreased by 41.44%, and the aEMG of the power values decreased by 36.61%. This result indicates a decrease in muscle activation power under the ON-Exo condition, implying that the upper limb exoskeleton offers a measurable assistive effect.

By comparing the EMG signal envelopes and time-domain features between the OFF-Exo and ON-Exo conditions, it is evident that the muscle activation power during loaded elbow flexion is lower when wearing the exoskeleton. This demonstrates that the upper limb exoskeleton robot offers effective assistance, reducing muscle activation levels with the exoskeleton's support. This can enhance the endurance of upper limb movements or be used for rehabilitation training for individuals with pathological upper limb weakness. Analysis of the EMG features of the biceps confirms the feasibility of the exoskeleton in providing assistance to the elbow joint.

2.1 Comprehensive performance evaluation

To comprehensively validate the effectiveness of the proposed upper limb exoskeleton, a systematic performance evaluation was conducted. Unlike the preliminary assessment based on individual user testing, the present evaluation involved a larger cohort by including five additional participants of varying ages, thereby enhancing the reliability of the study results. During the experiment, each participant performed ten single-arm elbow flexion tasks under load. Furthermore, subjective evaluations of comfort and ease of use were obtained through a structured participant questionnaire, with scores ranging from 1 to 5 (where higher scores indicate better user perception).

Table 2.
Time-domain feature comparison of EMG.

Time-domain feature		Collected value	Reduction rate	Power value	Reduction rate
RMS	OFF-Exo	94.32	41.61%	10.16	41.44%
	ON-Exo	55.07		5.95	
aEMG	OFF-Exo	58.92	35.79%	6.20	36.61%
	ON-Exo	37.83		3.93	

Source: authors

Table 3.
Summary of experimental data on the comprehensive performance evaluation for exoskeleton.

Participant ID	Age (years)	Height (cm)	Weight (kg)	ON-Exo (RMS)	OFF-Exo (RMS)	ON-Exo (aEMG)	OFF-Exo (aEMG)	Comfort Score (1-5)	Ease of Use Score (1-5)
P1	22	170	65	55.1	94.3	37.8	58.9	4	4
P2	24	175	70	54.8	93.5	36.5	57.5	4	5
P3	25	180	75	56.3	95.2	38.1	59.2	3	4
P4	28	165	62	53.2	92.6	36.2	56.3	5	4
P5	26	172	68	55.5	94.8	37.5	58.6	4	5

Source: authors

Table 3 presents a summary of the comprehensive performance evaluation data for the exoskeleton, including participants' anthropometric parameters, electromyographic signal metrics (RMS and aEMG) collected under both exoskeleton-assisted and unassisted conditions, as well as subjective ratings of comfort and ease of use. Each participant is assigned a unique identifier (ID), labeled from P1 to P5, where "P" denotes "Participant".

To further assess the sustained usability of the exoskeleton device, a long-term usability experiment was conducted, with a particular focus on the progression of users' perceived fatigue during continuous wear. In the test protocol, participants performed standardized upper limb tasks while periodically rating their subjective fatigue levels at predefined time intervals (5, 15, 30, 40, and 60 minutes). The fatigue scores were based on a 1–10 scale, with higher values indicating greater perceived fatigue. This score is positively correlated with the RMS measurement value.

As shown in Fig. 7, all five participants exhibited an upward trend in fatigue ratings over time, suggesting that prolonged use of the exoskeleton, even under assistive conditions, may lead to a gradual accumulation of muscular fatigue.

The primary objective of the exoskeleton is to provide assistive support and reduce muscular fatigue; however, it cannot entirely eliminate fatigue accumulation. As such, a gradual increase in perceived fatigue over time is a physiologically expected outcome during extended use. Notably, the subjective fatigue ratings were partially informed by trends observed in electromyographic signal metrics (RMS), thereby enhancing the reliability of fatigue assessment. For comparison, subjective fatigue ratings under non-assisted (no-exoskeleton) conditions were also collected and are presented in Fig. 8.

A comparison between Fig. 7 and Fig. 8 indicates that subjective fatigue scores were consistently lower when participants performed tasks with exoskeleton assistance, as opposed to the non-assisted condition. This suggests that the exoskeleton is effective in mitigating upper limb fatigue to a certain extent during repetitive motion tasks.

Finally, we conducted a systematic analysis of the limitations of the proposed upper limb exoskeleton in practical applications and proposed several feasible optimization strategies based on its current design characteristics. Although the upper limb exoskeleton exhibited satisfactory performance across the aforementioned core experimental evaluations, it still presents certain limitations in terms of accommodating a

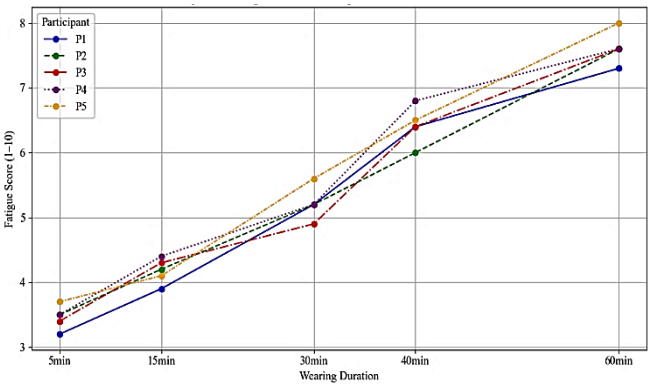

Figure 7. Subjective fatigue score curves of different participants using exoskeleton device.
Source: authors

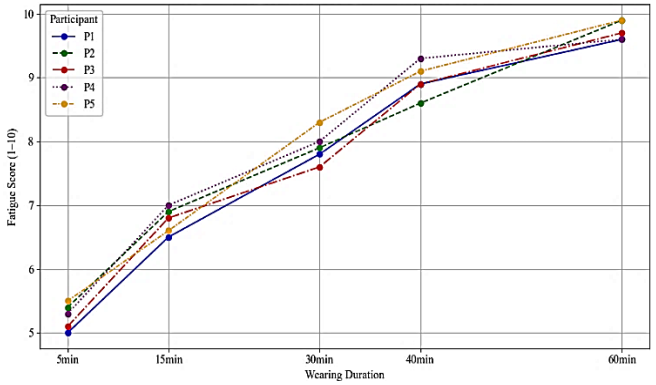

Figure 8. Subjective fatigue score curves of different participants without using exoskeleton devices.
Source: authors

wide range of user profiles. Specifically, when accommodating participant users with diverse body types (e.g., significant differences in height or weight) and varying levels of motor ability (e.g., individuals in early-stage rehabilitation versus healthy subjects), the device may encounter issues such as structural misalignment, inconsistent assistive effectiveness, and reduced wearing comfort. To enhance the individual adaptability and large-scale deployment potential of the upper limb exoskeleton system, future work will focus on adjustable structural design, dynamic regulation algorithms based on anthropometric parameters, and user state-aware feedback mechanisms. For example, modular or adaptive adjustment components could be introduced to accommodate variations in upper limb length and elbow joint axis alignment. In parallel, real-time optimization of control parameters using physiological data from the user could improve both wearing comfort and cooperative assistance performance. These improvements are expected to significantly extend the applicability of the proposed exoskeleton system across a range of scenarios, including clinical rehabilitation, human–robot collaboration, and industrial assistance.

1. Conclusion

This work proposes a low-cost, portable upper limb exoskeleton device that can be worn like a backpack, connecting to the wearer's back and arm. The device can alleviate the burden on the arm during lifting or carrying heavy objects and support rehabilitation training for patients with upper limb injuries in the later stages of elbow joint rehabilitation. The structural design of the exoskeleton is customized to align with the degrees of freedom of the human upper limb, offering flexible and smooth rotational freedom for each joint and delivering controllable assistive torque at the elbow joint. Additionally, passive support structures and active assistive motors improve the smoothness of elbow joint movements, enabling dual-motor torque feedback to enhance elbow assistance. To lower manufacturing costs and simplify production, most of the exoskeleton components were made using 3D printing with white resin. Safety is ensured by mechanical limits within the exoskeleton to restrict its workspace, keeping it within the normal range of human motion. The control strategy for the exoskeleton adopts a voltage-based FOC method with torque feedback that does not require current sampling. Synchronous rotation between the inner gimbal motor and the outer brushless motor, in conjunction with the forearm support board, enables the user to exert slight effort to achieve synchronized motor-driven assistance. This study seeks to improve upper limb endurance in specific populations, facilitating the recovery or enhancement of the wearer's motor function. Furthermore, it holds potential for advancing the development and adoption of upper limb exoskeleton robots, thereby increasing the accessibility and impact of these devices across diverse user groups.

References

[1] Siviy, C., Baker, L.M., Quinlivan, B.T. et al., Opportunities and challenges in the development of exoskeletons for locomotor assistance. Nature Biomedical Engineering,7(4), pp. 456-472, 2023. DOI: https://doi.org/10.1038/s41551-022-00984-1

[2] Zimmermann, Y., Sommerhalder, M., Wolf, P. et al., ANYexo 2.0: a fully actuated upper-limb exoskeleton for manipulation and joint-oriented training in all stages of rehabilitation. IEEE Transactions on Robotics, 39(3), pp. 2131-2150, 2023. DOI: https://doi.org/10.1109/TRO.2022.3226890

[3] Nassour, J., Zhao, G., and Grimmer, M., Soft pneumatic elbow exoskeleton reduces the muscle activity, metabolic cost and fatigue during holding and carrying of loads. Scientific Reports,11(1), art. 12556, 2021. DOI: https://doi.org/10.1038/s41598-021-91702-5

[4] Georgarakis, A-M., Xiloyannis, M., Wolf, P., et al., A textile exomuscle that assists the shoulder during functional movements for everyday life. Nature Machine Intelligence, 4(6), pp. 574-82, 2022. DOI: https://doi.org/10.1038/s42256-022-00495-3

[5] Walsh, C.J., Paluska, D., Pasch, K., et al., Development of a lightweight, under. actuated exoskeleton for load-carrying augmentation, in: Proceedings 2006 IEEE International Conference on Robotics and Automation, 2006 ICRA, 2006, pp. 15-19. DOI: https://doi.org/10.1109/ROBOT.2006.1642234

[6] Wu, K.Y., Su, Y.Y., Yu, Y.L., et al., A 5-Degrees-of-freedom lightweight elbow-wrist exoskeleton for forearm fine-motion rehabilitation. IEEE/ASME Transactions on Mechatronics, 24(6), pp. 2684-2695, 2019. DOI: https://doi.org/10.1109/TMECH.2019.2945491

[7] Collins, S.H, Wiggin, M.B., and Sawicki, G.S., Reducing the energy cost of human walking using an unpowered exoskeleton. Nature, 522(7555), pp. 212-215, 2015. DOI: https://doi.org/10.1038/nature14288

[8] Li, H., Sui, D., Ju, H., et al., Mechanical compliance and dynamic load isolation design of lower limb exoskeleton for locomotion assistance. IEEE/ASME Transactions on Mechatronics, 27(6), pp. 5392-5402, 2022. DOI: https://doi.org/10.1109/TMECH.2022.3181261

[9] Gull, M.A., Bai, S., and Bak, T., A Review on Design of Upper Limb Exoskeletons. 9(1), art, 9010016, 2020. DOI: https://doi.org/10.3390/robotics9010016

[10] Kim, H., and Asbeck, A.T., Just noticeable differences for elbow joint torque feedback. Scientific Reports, 11(1), art. 23553, 2021. DOI: https://doi.org/10.1038/s41598-021-02630-3

[11] Kim, H., and Asbeck, A.T., The effects of torque magnitude and stiffness in arm guidance through joint torque feedback. IEEE Access, 10, pp. 5842-5854, 2022. DOI: https://doi.org/10.1109/ACCESS.2022.3141981

[12] Vitiello, N., Lenzi, T., Roccella, S., et al., NEUROExos: a powered elbow exoskeleton for physical rehabilitation. IEEE Transactions on Robotics, 29(1), pp. 220-235, 2013. DOI: https://doi.org/1109/TRO.2012.2211492

[13] Kim, H., and Asbeck, A.T., An elbow exoskeleton for haptic feedback made with a direct drive hobby motor. HardwareX, 8, art. e00153, 2020. DOI: https://doi.org/10.1016/j.ohx.2020.e00153

[14] Perry, J.C., Rosen, J., Burns, S., Upper-Limb powered exoskeleton design. IEEE/ASME Transactions on Mechatronics, 12(4), 408-417, 2007. DOI: https://doi.org/10.1109/TMECH.2007.901934

[15] Abassi, M., Khlaief, A., Saadaoui, O., et al., Performance analysis of FOC and DTC for PMSM drives using SVPWM technique, in: Proceedings of the 2015 16th International Conference on Sciences and Techniques of Automatic Control and Computer Engineering (STA), 2015, pp. 21-23. DOI: https://doi.org/10.1109/STA.2015.7505167

[16] Pinto-Fernandez, D., Torricelli, D., Sanchez-Villamanan, M.D.C., et al., Performance evaluation of lower limb exoskeletons: a systematic review. IEEE Transactions on Neural Systems and Rehabilitation Engineering, 28(7), pp. 1573-1583, 2020. DOI: https://doi.org/10.1109/TNSRE.2020.2989481

[17] Z. Du, et al., Mechanical design and preliminary performance evaluation of a passive arm-support exoskeleton, 2020 IEEE/RSJ International Conference on Intelligent Robots and Systems (IROS), pp. 3371-3376, 2020. DOI: https://doi.org/10.1109/IROS45743.2020.9341290

[18] Liu, Y., Li, X., Zhu, A., Zheng, Z., and Zhu, H., Design and evaluation of a surface electromyography-controlled lightweight upper arm exoskeleton rehabilitation robot. International Journal of Advanced Robotic Systems. 18(3), art. 003461, 2021. DOI: https://doi.org/10.1177/17298814211003461

J. Huang, received his BSc. Eng. in Mechanical Engineering in 2023. He is currently pursuing a Master's degree at the School of Mechanical Engineering, Jiangnan University, China. His research interests include: exoskeleton and humanoid robot, fractal gripper and robotic manipulator, imitation learning and reinforcement learning, and generative machine learning.
ORCID: 0009-0005-3544-2655

F. Wu, is currently pursuing the BSc. degree in Mechanical Engineering at Jiangnan University, Wuxi, China. His research interests include exoskeletons, robot control, and bionic devices.
ORCID:0009-0005-6454-2540

B. Ding, entered the School of Mechanical Engineering at Jiangnan University in 2022 to pursue a bachelor's degree. Her research interests include: portable upper limb rehabilitation exoskeleton robots based on deep learning, exoskeleton modeling, and product function testing.
ORCID:0009-0007-1703-8725

J. Yin, studied in the major of Packaging Engineering at the School of Mechanical Engineering, Jiangnan University from September 2022 to June 2026. His research interests include embodied intelligence and the preparation of high-barrier plastic films.
ORCID:0009-0007-6312-6531

G. Yang, received his admission to Jiangnan University in 2022 and is currently a third-year undergraduate student majoring in Robotics Engineering at the same institution. His academic interests include: exoskeleton robot structural design; deep learning algorithm optimization; robotic motion capture; human-machine interaction systems for assistive technologies.
ORCID:0009-0001-4933-6205

Z. Song, received his BSc. from Beihang University in 2011 and his PhD. from Tsinghua University in 2016. Since 2022, he has been with Jiangnan University, China, where he is currently a Professor at the School of Mechanical Engineering. His research interests include: anomaly detection and 3D reconstruction based on machine vision, intelligent control in humanoid robotics and smart equipment, and multiscale modeling using machine learning.
ORCID: 0000-0002-8615-868X